THE JOURNAL OF PHYSICAL CHEMISTRY C
A JOURNAL OF THE AMERICAN CHEMICAL SOCIETY

pubs.acs.org/JPCC

Article

Influence of Structural Dynamics on the Kinetics of Atomic Hydrogen Reactivity with Low-Temperature Alkanethiolate Self-Assembled Monolayers

Published as part of The Journal of Physical Chemistry virtual special issue "Daniel Neumark Festschrift".

Sarah Brown, Jeffrey D. Sayler, and S. J. Sibener*

Cite This: https://doi.org/10.1021/acs.jpcc.1c07487

Read Online

ACCESS | Metrics & More | Article Recommendations

ABSTRACT: This study examines the impact of surface temperature on alkanethiolate self-assembled monolayer (SAM) reactivity with atomic hydrogen (H) as well as how the combined effects of temperature and alkanethiol chain length alter the reaction outcome. This is achieved using ultrahigh vacuum scanning tunneling microscopy (UHV-STM) to monitor the spatiotemporal evolution of the monolayer throughout the reaction. We find that with decreasing temperature, the reaction rate of alkanethiol SAMs with atomic H decreases monotonically. Furthermore, the kinetic profile of the low-temperature reaction differs from that at room temperature, indicating structural and dynamical fluctuations within the monolayer that influence reactivity. Chain length is also seen to significantly affect reactivity at reduced substrate temperature, with longer alkanethiols reacting more slowly than shorter ones. Finally, we observe a unique surface rearrangement of the SAM upon exposure to atomic H, including changes in the organization of close-packed thiol domains and the evolution of gold adatom islands not observed at elevated temperatures. Overall, this work provides both quantitative and nanoscopic insight into how substrate temperature influences the structural dynamics of thiolate monolayers and how these fluctuations influence chemical reactivity.

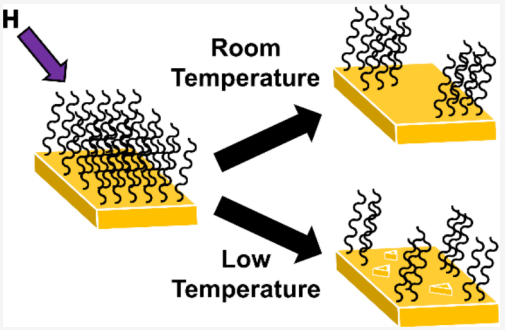

1. INTRODUCTION

The ability to passivate a chemically active surface is of interest to many industrial sectors such as metallurgy and semiconductor manufacturing, as the functional lifetime of these materials depends heavily on slowing their degradation when they are exposed to a variety of reactive species. To this end, organic thin films demonstrate significant promise in their use as passivating coatings for metal and semiconductor surfaces. Thiolate self-assembled monolayers (SAMs), for example, have already been shown to provide significant resistance to chemical reactivity and corrosion on a variety of technologically relevant substrates.[1−8]

However, structural deviations often occur in these films under different environmental conditions, which can alter their physical and chemical properties and, in turn, impact their passivation abilities. For example, many pioneering studies on alkanethiolate SAMs on Au(111), both theoretical[9−12] and experimental,[13−15] show that these films are subject to temperature-dependent tilt-order phase transformations due to their canted assembly on the surface. These include both low-temperature transitions (T < 300 K) between two ordered phases of differing tilt angles, and high-temperature transitions (T > 300 K) between ordered, crystalline phases and phases characterized by disordered molecular fluctuations. Further studies also illustrate that the surface structure and packing density of alkanethiolate SAMs influence the energy-transfer dynamics that occur between a monolayer and gas-phase particles that collide with it.[16,17] A thorough understanding of how structural changes impact surface reactivity is hence crucial in advancing the implementation of functional thin films in real-world applications.

The well-characterized and highly ordered polycrystalline structure of thiolate SAMs, in addition to their vast chemical versatility, provides a unique platform for studying the dynamics between environmental conditions and chemical reactivity of organic thin films.[18−21] Several groups have employed spectroscopic techniques such as X-ray photoelectron spectroscopy[22] and reflection absorption infrared spectroscopy[23] to examine how surface temperature influences

Received: August 23, 2021
Revised: October 8, 2021

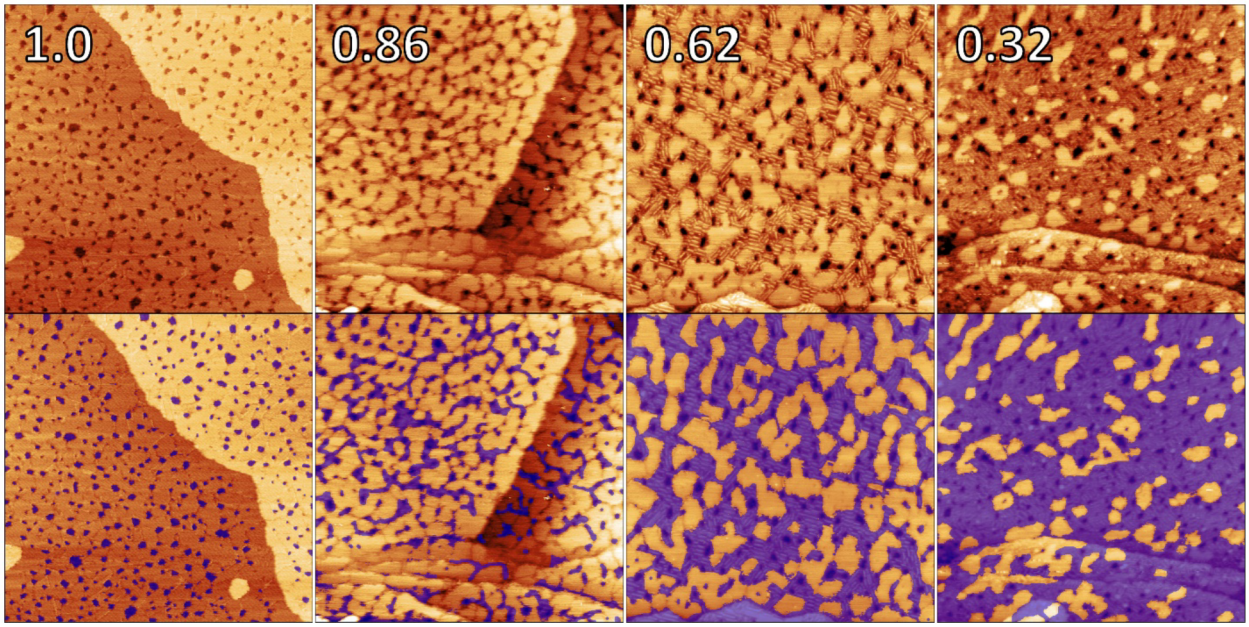

Figure 1. Representative STM image progression (200 nm × 200 nm) of a 1-octanethiolate (8C) SAM as it reacts with atomic H at 250 K. Top row: STM images showing φ-phase coverages of 100%, 86%, 62%, and 32%. Regions of low-density SAM first appear around the domain boundaries at 86% coverage, with low-density striped phase clearly visible beginning at 62% coverage. Bottom row: examples of the image processing procedure used to quantify the φ-phase coverage for each of the images in the top row, with the low-density SAM regions marked in blue and the φ-phase domains in orange. Note that initial defect sites such as etch pits and grain boundaries are always masked.

the film structure and reactivity of SAMs with O(^{3}P). Previous work has also utilized a combination of spectroscopies to explore the impact of substrate temperature on alkanethiolate interactions with X-ray irradiation.[24]

To gain an accurate understanding of how these temperature-dependent thin film dynamics evolve on the nanoscale, however, we must use a more localized experimental technique such as scanning probe microscopy (SPM). SPM allows us to better investigate kinetic events on the molecular level, rather than being limited to averaged information from the entire reactive surface. This work therefore uses ultrahigh vacuum scanning tunneling microscopy (UHV-STM) to investigate the localized impact of substrate temperature and alkanethiol chain length on self-assembled monolayer reactivity. First, we track the reaction progression of 1-decanethiolate (10C) SAMs exposed to atomic hydrogen (H) at substrate temperatures T_S = 295, 270, 250, and 130 K by monitoring the close-packed thiol surface coverage. Using our previously developed rate model,[25] we describe the reaction kinetics and deduce the rate constants for the reaction at each temperature. Furthermore, we compare the reactivity of 1-octanethiolate (8C) and 10C SAMs at low temperature (250 K) to reveal the combined effects of reduced T_S and shorter chain length on reaction kinetics with atomic H. Finally, we examine the impact of substrate temperature on the SAMs' surface rearrangement during their reaction with atomic H. This paper provides significant insight into the relationship between substrate temperature and the resultant chemical activity of organic thin films upon exposure to energetic species such as atomic H. In particular, it emphasizes how structural fluctuations in the film influence its reactivity as a function of temperature.

2. EXPERIMENTAL SECTION

Experiments are performed in a UHV chamber (base pressure $\lesssim 5 \times 10^{-10}$ Torr) that houses both an RHK 350 Beetle UHV-STM/AFM and a Mantis MGC-75 thermal gas cracker.[25] The *in situ* gas cracker is located 80 mm from the sample and oriented 50° from the imaging stage's surface normal, occupying a solid angle of 0.004 sr. All atomic H flow therefore arrives at the surface from the same direction, and the impinging beam is controlled by a manual shutter.

The gas cracker produces atomic H by passing molecular hydrogen (backing pressure of 1×10^{-7} Torr) through a heated iridium capillary and subsequently collimating it. Under these conditions, the expected cracking efficiency and atomic H flux are 90%[26] and ~10^{12} H atoms cm^{-2} s^{-1}, respectively. To prevent shadowing from the STM tip, we fully retract the microscope head from the sample during exposures.

We prepare our thiolate SAMs using solution deposition on flame-annealed Au(111)-on-mica substrates from Phasis. The substrates are immersed in 1.0 mM solutions of 1-octanethiol (8C) and 1-decanethiol (10C) in ethanol for 24 h at room temperature and 2.5 h at 60 °C, respectively. Samples are then rinsed with ethanol and dried in air prior to placement in the UHV chamber.

For experiments at T_S < 295 K, the STM sample stage is cooled with liquid nitrogen using a flow cryostat. A stable sample temperature is maintained using a radiative heating feedback loop and measured with a Type K thermocouple.

All STM images are taken with a +0.70 V bias on the sample and a tunneling current set point of 10 pA. Previous control experiments with 10C SAMs confirm that exposure to atomic H is uniform across the entire substrate and that there are no noticeable differences in reactivity due to variations in Au(111) surface structure or SAM domain orientation for this reaction.[25] Finally, we perform all of our STM image processing using Gwyddion, an open-source software for SPM data analysis.[27]

https://doi.org/10.1021/acs.jpcc.1c07487
J. Phys. Chem. C XXXX, XXX, XXX−XXX

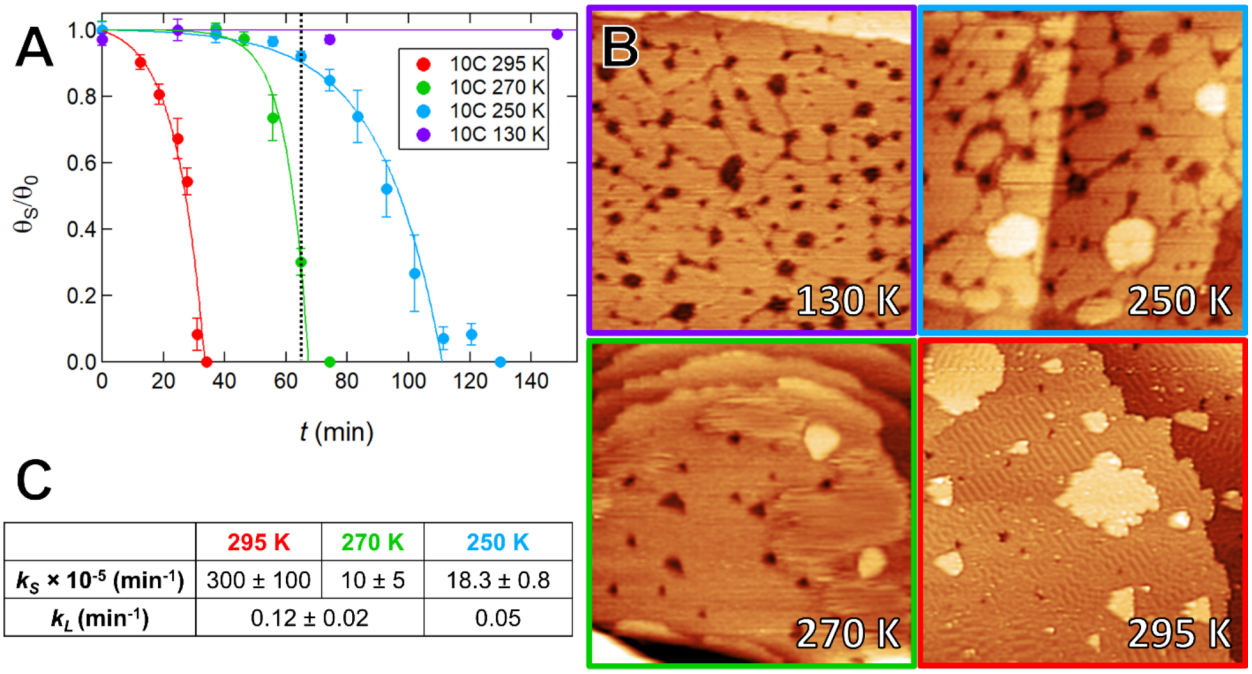

C

	295 K	270 K	250 K
$k_S \times 10^{-5}$ (min^{-1})	300 ± 100	10 ± 5	18.3 ± 0.8
k_L (min^{-1})	0.12 ± 0.02		0.05

Figure 2. (A) Plot showing the fraction of 1-decanethiolate (10C) SAM φ-phase coverage as a function of atomic H exposure time, at four different temperatures and under constant atomic H flux. Each point is a weighted average of the data collected for the sample at that time, and we performed multiple experimental runs to confirm the validity of the trajectories. Solid curves are fits produced using eq 1, and the vertical dashed line marks the time at which we obtained the images in (B). (B) Representative images (150 nm × 150 nm) of 10C SAMs at 130, 250, 270, and 295 K after 64 min of atomic H exposure. At this time point, we observe a wide range of temperature-dependent reactivity: the SAM at 130 K shows little-to-no reactivity (thin grain boundaries with numerous evenly distributed etch pits), whereas the SAM at 295 K is fully reacted (covered in striped low-density phase and covered in bright gold islands). (C) Table of rate constants produced by eq 1 for all four reaction temperatures. Although the two-rate model appears to adequately describe the reaction at 295 and 270 K, there is breakdown at 250 K, as evidenced by a significantly lower value for k_L.

3. RESULTS AND DISCUSSION

It is well-documented in previous studies[28] that the primary reaction mechanism of atomic H with short-chain alkanethiolate SAMs (C ≤ 12) is through the cleavage of the sulfur−gold bonds, thereby removing entire thiols from the surface. This reactivity, as shown in our reaction of an 8C SAM in Figure 1, initially appears around the thiolate domain grain boundaries and subsequently expands outward, in agreement with previous results.[25,29−33] The removal of thiolate molecules promotes the formation of various low-density phases, including both ordered lying-down, or striped, phases and disordered 2D fluids.[34−37] These low-density regions continue to grow as the reaction proceeds, consuming the hexagonal close-packed (φ-phase) domains until only low-density alkanethiol and gold adatom islands[25,29,30] remain. We consider the reaction to be complete when no φ-phase SAM is left on the Au(111) surface.[25] The bottom row of Figure 1 illustrates the image processing procedure used to quantify the φ-phase coverage at any point in the reaction, where all low-density SAM regions are masked in blue to allow the computation of the unreacted area.

The results of our study are divided into three parts. First, we present the reaction of 1-decanethiolate (10C) SAMs at decreased substrate temperatures and discuss the validity of our previously developed kinetic model[25] for $T_S \neq 295$ K. Second, we examine the effect of chain length on low-temperature alkanethiolate reactivity by comparing the reaction rates of 8C and 10C SAMs at both T_S = 295 and 250 K. Finally, we analyze the impact of T_S on nanoscale alkanethiolate surface rearrangement, with particular emphasis on the restructuring of φ-phase domains and gold adatom islands at low temperature.

3.1. 1-Decanethiolate (10C) Reactivity at Various T_S.

To understand the impact of reduced temperature on alkanethiolate SAM reactivity with atomic H, we tracked the reaction progression of 10C SAMs at T_S = 295, 270, 250, and 130 K. These results are presented in Figure 2A, where the area fraction of φ-phase SAM is plotted as a function of hydrogen exposure time. The rate of a 10C SAM's reaction with atomic H decreases with decreased temperature, with the lowest temperature of T_S = 130 K showing no measurable reaction. This trend in reactivity in relation to T_S is in agreement with previous work[22−24] and is visually represented in Figure 2B, where the STM images of 10C SAMs are presented for the same atomic H exposure at different surface temperatures.

The experimental data in Figure 2A were fitted to our previously developed model, which successfully describes the reactivity of alkanethiolate SAMs of different lengths at room temperature[25]

$$\frac{\theta_S}{\theta_0} = Ae^{-(k_S - k_L)t} + \frac{1}{1 - \frac{k_S}{k_L}} \quad (1)$$

where $\frac{\theta_S}{\theta_0}$ is the normalized area fraction of φ-phase SAM, t is the hydrogen exposure time, k_S is the rate constant for hydrogen's reaction with the φ-phase, k_L defines the rate of hydrogen's reaction with low-density phases, and A is a constant dependent on k_S and k_L. This two-rate model builds

https://doi.org/10.1021/acs.jpcc.1c07487
J. Phys. Chem. C XXXX, XXX, XXX−XXX

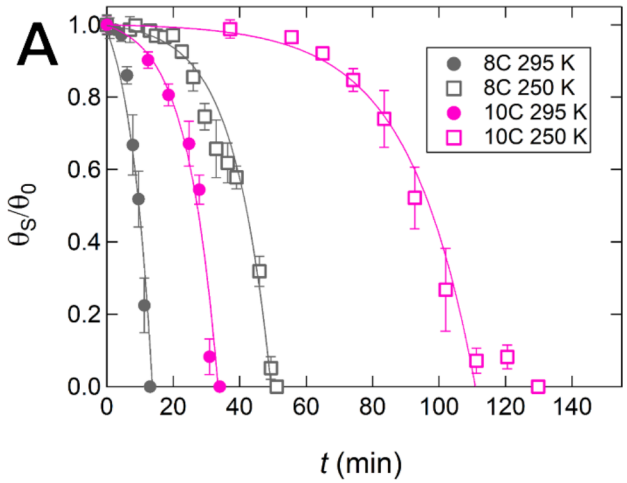

B

295 K ●

	8C	10C
$k_S \times 10^{-5}$ (min^{-1})	2200 ± 200	300 ± 100
k_L (min^{-1})	0.13 ± 0.03	

250 K □

	8C	10C
$k_S \times 10^{-5}$ (min^{-1})	89 ± 3	18.3 ± 0.8
k_L (min^{-1})	0.07 ± 0.02	

Figure 3. (A) Plot showing the fraction of φ-phase coverage as a function of atomic H exposure time for 8C and 10C SAMs at 295 and 250 K. Each point is a weighted average of the data collected for the sample at that time, and solid curves are fits produced using eq 1. (B) Tabulated rate constants produced by eq 1 for 8C and 10C SAMs at 295 and 250 K. We note that k_L's independence of chain length appears to persist even at low temperature.

on previously proposed theory[38] and assumes that the reaction of thiols with atomic H occurs one of two ways: (a) the slow reaction of sterically hindered close-packed thiols or (b) the fast reaction of easily accessible edge-site and/or low-density thiols. Calculated reaction probabilities based on the atomic H flux and time-dependent SAM densities also provide further support for our two-rate model. At T_S = 295 K, a 10C SAM has ~30% reaction probability for $\frac{\theta_S}{\theta_0}$ = 0.95, which increases to a ~90% reaction probability once there is greater low-density thiol coverage and $\frac{\theta_S}{\theta_0}$ = 0.60.

Both the fitted curves in Figure 2A and the rate constants in Figure 2C show that the two-rate model describes the experimental data well for T_S = 295 and 270 K adequately. Three key statements about the impact of temperature on the reaction can be made following this analysis: First, k_L varies minimally between the two temperatures, which implies that the lying-down phase is equally reactive under both conditions, and thus the reactions likely follow similar mechanisms. Second, $k_L \gg k_S$, which once again suggests that low-density phase thiols are significantly more reactive than φ-phase thiols, regardless of temperature. Finally, k_S decreases for colder samples, which confirms that atomic H's ability to permeate the φ-phase domains is greatly reduced due to increased SAM crystallinity at lower temperature.[9−11,14,23,24]

However, the proposed two-rate model disagrees with the experimental data for $T_S \leq$ 250 K. As shown in Figure 2A, there is a modest divergence of the model fit from the experimental data at longer atomic H exposure times. Unlike the reactions at T_S = 295 and 270 K, which accelerate continuously after their incubation periods, the reaction at T_S = 250 K appears to slow down as it approaches completion. This observation is a direct consequence of lingering φ-phase domains on the surface near the end of the reaction and is reflected in the calculated reaction probabilities for a 10C SAM at T_S = 250 K. For $\frac{\theta_S}{\theta_0}$ = 0.63, the reaction probability is at its peak of ~31%; however, for $\frac{\theta_S}{\theta_0}$ = 0.17, it drops to ~18% and continues to decrease until the end of the reaction. Sigmoidal profiles like these are commonly observed in systems governed by the Avrami equation, where the reaction begins slowly, accelerates when multiple nucleation centers are available to react simultaneously, and then decelerates once the amount of available reactant becomes minimal. In our experiment, we propose that the final deceleration occurs when the φ-phase domains approach the minimum size for thermodynamic stability, but there is not yet enough available surface area for all of the φ-phase to convert into lower-density striped phases. This phenomenon is more probable at lower temperature because the thiols are less mobile on the Au(111) surface, which prohibits the φ-phase from coalescing into larger and more stable domains.[36,39] Previous work supports this proposal, using the Avrami theorem as a basis to describe both the formation process of a self-assembled monolayer from solution[40] and the reductive desorption of alkanethiols from an Au(111) surface.[41]

The change in experimentally observed reactivity at T_S = 250 K supports the conclusions drawn by past molecular dynamics studies,[9−11] which state that alkanethiolate SAMs undergo distinct structural phase transitions at specific temperatures. At T_S = 150 K, thiolate SAMs form highly ordered solid films with all molecules tilted unidirectionally at ~34° from surface normal[14] and rotational motion fully prohibited. Conversely, at $T_S \geq$ 300 K the collective tilt angle becomes diffuse, and the molecular fluctuations increase significantly. However, for 250 K $\leq T_S \leq$ 300 K, there exists an intermediate phase where although crystalline order is largely maintained, molecular fluctuations appear in the individual molecules' tilt directions. This suggests that our observed difference in reactivity at T_S = 250 K compared to T_S = 270 and 295 K can be explained by differences in the monolayer's temperature-dependent dynamic disorder and the degree of molecular fluctuations experienced, which in turn influences atomic H mobility through the film.

3.2. Effect of Chain Length on Low-Temperature Alkanethiolate Reactivity. We also investigated how the chain length dependence of alkanethiolate reactivity is affected at low T_S by comparing the reaction progression of 8C and 10C SAMs at T_S = 295 and 250 K. Figure 3A plots the area fraction of φ-phase SAM as a function of hydrogen exposure time, and the experimental data are fitted to eq 1. We find that

https://doi.org/10.1021/acs.jpcc.1c07487
J. Phys. Chem. C XXXX, XXX, XXX−XXX

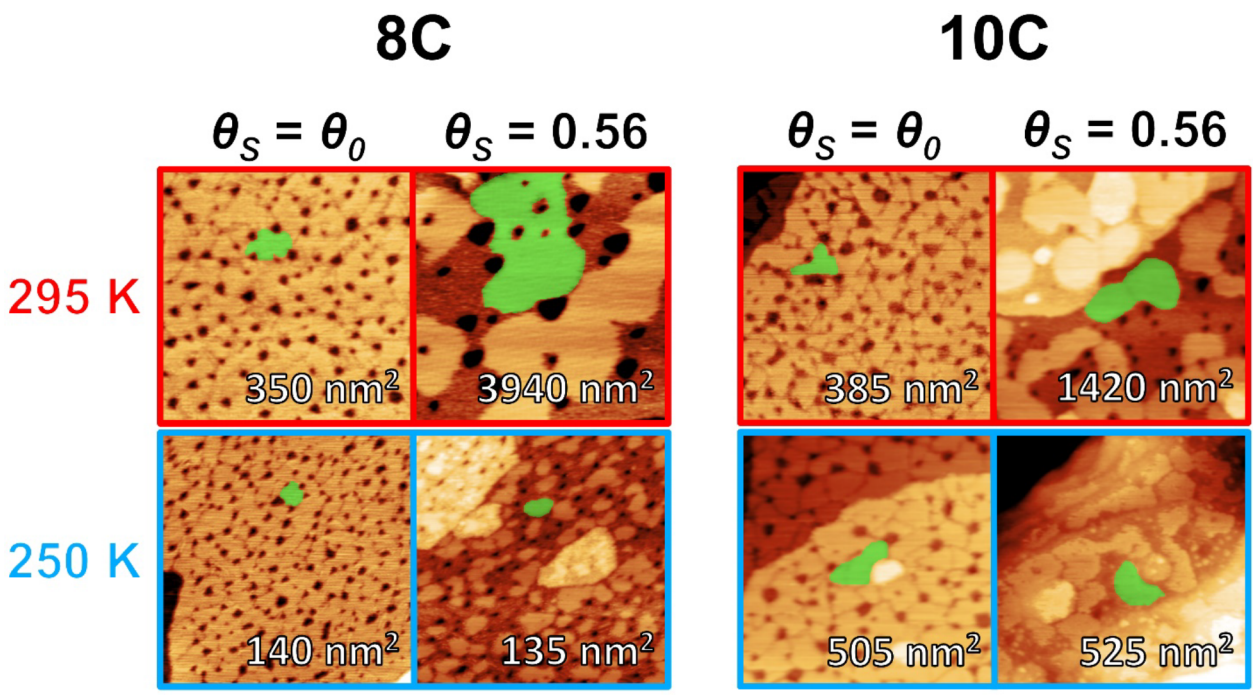

Figure 4. STM images (150 nm × 150 nm) of 8C and 10C SAMs at T_S = 295 and 250 K, both prior to reaction and at θ_S = 0.56. Each image shows a representative φ-phase domain highlighted in green as well as the average φ-phase domain size for that chain length, temperature, and surface coverage in the bottom right-hand corner. At T_S = 295 K, the average φ-phase domain size increases as the reaction progresses, with the 8C sample exhibiting greater rearrangement than the 10C sample. At T_S = 250 K, however, the φ-phase domains remain approximately the same size following exposure to atomic H. This phenomenon is attributed to the freezing of lateral molecular movement, which would typically be thermodynamically favorable, at reduced temperature.

the shorter SAM reacts with atomic H more quickly than the longer SAM because longer alkanethiolate chains exhibit a more crystalline packing structure and are thus less penetrable to atomic H.[28,42,43] This observation is true at both experimental temperatures, and the rate constants for each fit are tabulated in Figure 3B.

Both the 8C and 10C SAMs exhibit a similar decrease of 95% in relative reaction rate at T_S = 250 K compared to T_S = 295 K. This suggests that although the SAMs' reaction with atomic H is chain-length-dependent across multiple substrate temperatures, any changes in alkanethiolate packing due to reduced T_S are comparable for 8C and 10C SAMs. Although some previous studies[23] show that lowering T_S yields a more severe relative decrease in reactivity for longer-chain thiols, we suspect that this difference only manifests when comparing SAMs across different chain length regimes. Because both 8C and 10C SAMs are classified as short-chain alkanethiols (C ≤ 12),[28] as determined by their tilt structure,[15] we expect the temperature dependences of their packing behavior and reactivity to be relatively similar.

3.3. Impact of T_S on Nanoscale Alkanethiolate Surface Rearrangement. Finally, we use the nanoscale imaging capabilities of STM to analyze chain-length-dependent surface rearrangements[25] at low T_S during reaction with atomic H. These temperature-dependent differences in surface morphology result in the rearrangement of φ-phase domains and etch pits and the evolution of gold adatom islands.

First, Figure 4 presents STM images at both $\theta_S = \theta_0$ and θ_S = 0.56 and demonstrates how the φ-phase domains of 8C and 10C SAMs evolve during the course of reaction at T_S = 295 and 250 K. At room temperature, we observe the anticipated Ostwald ripening of the close-packed thiols and etch pits,[25] with the 8C sample exhibiting greater rearrangement than the 10C sample. The chain length dependence of the monolayer restructuring is attributed to the van der Waals forces between neighboring alkanethiol molecules; the shorter the molecule, the weaker the intermolecular forces within the film[28] and therefore the greater the molecular mobility on the Au(111) surface. At T_S = 250 K, however, neither 8C nor 10C SAMs exhibit a statistically significant difference in their average φ-phase domain size when comparing $\theta_S = \theta_0$ to θ_S = 0.56; that is, at low temperature, the φ-phase domains of alkanethiolate SAMs remain approximately the same size throughout their reaction with atomic H, as illustrated by the domains highlighted in green in Figure 4. We propose that this lack of surface rearrangement at T_S = 250 K is due to the thiols' reduced mobility at colder temperatures; the lower temperature prohibits molecular movement that would otherwise result in the formation of larger and more thermodynamically favorable domains.[36,39]

Finally, the temperature dependence of gold adatom island formation following the SAMs' exposure to atomic H is shown in Figure 5. During experiments performed at T_S = 295 K, gold islands appear exclusively at the end of the reaction; their appearance signals that the reaction with atomic H is complete and that no φ-phase SAM remains on the surface. This observation is also true for SAMs exposed to atomic H at T_S = 270 K. However, at T_S = 250 K, the gold islands appear gradually throughout the reaction, even while close-packed thiols are still present on the Au(111) surface. We propose that the slow growth of gold islands is partially due to the reduced mobility of thiols on the Au(111) surface at low temperature, although it is interesting to note that the Kandel group has also recently reported on similar reaction-induced surface evolution

https://doi.org/10.1021/acs.jpcc.1c07487
J. Phys. Chem. C XXXX, XXX, XXX−XXX

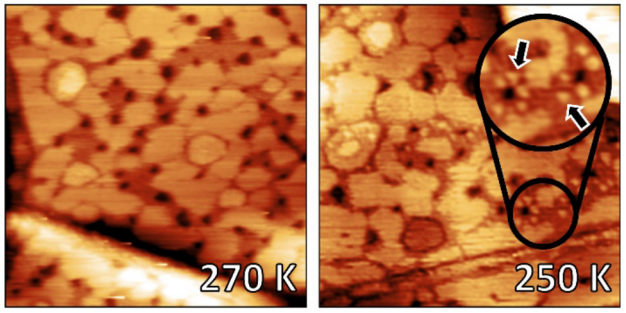

Figure 5. STM images (150 nm × 150 nm) of 10C SAMs with θ_S = 0.74 φ-phase coverage at 270 and 250 K. At 270 K, we observe the typical reaction progression: a widening of grain boundaries around the close-packed thiol domains. However, at 250 K, we notice the appearance of gold islands (see features highlighted in inset) within the low-density thiol regions, despite there still being φ-phase on the surface. This phenomenon occurred for both 10C and 8C SAMs at 250 K.

at higher temperatures than our results.[44] This suggests that other factors likely impact the rate of gold adatom growth, such as atomic H flux and overall reaction speed.

4. CONCLUSIONS

In this paper, we use STM to demonstrate that the temperature of alkanethiolate SAMs significantly impacts their reactivity with atomic H, in terms of both kinetics and surface reconstruction. First, our experimental data show that SAMs react more slowly as temperature decreases, and all reactivity can be eliminated at sufficiently low T_S. For slightly decreased temperatures (T_S = 270 K), the reaction kinetics are well-described using our previously developed two-rate model.[25] However, at T_S = 250 K, our proposed model diverges from the experimental data, likely due to a structural phase transition in the alkanethiol monolayer[9−11] which decreases the degree of molecular fluctuations experienced and, hence, hinders the mobility of atomic H through the SAM. Second, we find that shorter SAMs react with atomic H more quickly than longer SAMs due to increased dynamical fluctuations caused by their weaker interchain attractions,[28,42,43] and that this is true at both T_S = 295 and 250 K. Furthermore, 8C and 10C SAMs exhibit a similar decrease of 95% in relative reaction rate at T_S = 250 K compared to T_S = 295 K. These conclusions imply that although the SAMs' reaction with atomic H is chain-length-dependent at any given substrate temperature, changes in alkanethiolate packing due to reduced T_S are comparable for octanethiolate and decanethiolate SAMs. Finally, we observe nanoscale differences in the reaction-induced structural rearrangement of the alkanethiolate monolayers at T_S = 295 K compared to T_S = 250 K. At room temperature, the φ-phase domains undergo Ostwald ripening during their reaction with atomic H, with the 8C sample exhibiting greater rearrangement than the 10C sample. However, at T_S = 250 K, the average φ-phase domain size remains approximately unchanged following exposure to atomic H, for both the 8C and 10C SAMs. This lack of surface rearrangement is attributed to the reduced molecular motion of thiols across the surface at colder temperatures. Additionally, we observe a temperature dependence in the formation of gold adatom islands during the SAMs' reactions with atomic H. At room temperature, the adatoms appear abruptly after the φ-phase domains are gone; however, at T_S = 250 K, the adatoms grow slowly throughout the course of the reaction. We propose that this slow growth of gold islands is partially due to the reduced mobility of thiols on the Au(111) surface at low temperature, although it is also likely impacted by other factors such as atomic H flux and overall reaction speed. This STM study therefore yields important insight into temperature-dependent structural changes that occur in organic thin films, as well as how these rearrangements influence the films' chemical reactivity and passivation capabilities.

AUTHOR INFORMATION

Corresponding Author

S. J. Sibener − *The James Franck Institute and Department of Chemistry, The University of Chicago, Chicago, Illinois 60637, United States;* orcid.org/0000-0002-5298-5484; Email: s-sibener@uchicago.edu

Authors

Sarah Brown − *The James Franck Institute and Department of Chemistry, The University of Chicago, Chicago, Illinois 60637, United States*

Jeffrey D. Sayler − *The James Franck Institute and Department of Chemistry, The University of Chicago, Chicago, Illinois 60637, United States*

Complete contact information is available at: https://pubs.acs.org/10.1021/acs.jpcc.1c07487

Notes

The authors declare no competing financial interest.

ACKNOWLEDGMENTS

This work was supported by the National Science Foundation (Grant CHE-1900188). Support from the NSF-Materials Research Science and Engineering Center at the University of Chicago (Grant NSF-DMR-2011854) is also gratefully acknowledged.

REFERENCES

(1) Laibinis, P. E.; Whitesides, G. M. Self-Assembled Monolayers of n-Alkanethiolates on Copper Are Barrier Films That Protect the Metal against Oxidation by Air. *J. Am. Chem. Soc.* **1992**, *114* (23), 9022−9028.

(2) Robinson, G. N.; Freedman, A.; Graham, R. L. Reactions of Fluorine Atoms with Self-Assembled Monolayers of Alkanethiolates. *Langmuir* **1995**, *11* (7), 2600−2608.

(3) Scherer, J.; Vogt, M. R.; Magnussen, O. M.; Behm, R. J. Corrosion of Alkanethiol-Covered Cu(100) Surfaces in Hydrochloric Acid Solution Studied by in-Situ Scanning Tunneling Microscopy. *Langmuir* **1997**, *13* (26), 7045−7051.

(4) Burleigh, T. D.; Gu, Y.; Donahey, G.; Vida, M.; Waldeck, D. H. Tarnish Protection of Silver Using a Hexadecanethiol Self-Assembled Monolayer and Descriptions of Accelerated Tarnish Tests. *Corrosion* **2001**, *57* (12), 1066−1074.

(5) Jennings, G. K.; Yong, T.-H.; Munro, J. C.; Laibinis, P. E. Structural Effects on the Barrier Properties of Self-Assembled Monolayers Formed from Long-Chain ω-Alkoxy-n-Alkanethiols on Copper. *J. Am. Chem. Soc.* **2003**, *125* (10), 2950−2957.

(6) Lim, H.; Carraro, C.; Maboudian, R.; Pruessner, M. W.; Ghodssi, R. Chemical and Thermal Stability of Alkanethiol and Sulfur Passivated InP(100). *Langmuir* **2004**, *20* (3), 743−747.

(7) Tortech, L.; Mekhalif, Z.; Delhalle, J.; Guittard, F.; Géribaldi, S. Self-Assembled Monolayers of Semifluorinated Thiols on Electrochemically Modified Polycrystalline Nickel Surfaces. *Thin Solid Films* **2005**, *491* (1), 253−259.

(8) McGuiness, C. L.; Shaporenko, A.; Zharnikov, M.; Walker, A. V.; Allara, D. L. Molecular Self-Assembly at Bare Semiconductor Surfaces: Investigation of the Chemical and Electronic Properties of the Alkanethiolate-GaAs(001) Interface. *J. Phys. Chem. C* **2007**, *111* (11), 4226−4234.
(9) Hautman, J.; Klein, M. L. Molecular Dynamics Simulation of the Effects of Temperature on a Dense Monolayer of Long-chain Molecules. *J. Chem. Phys.* **1990**, *93* (10), 7483−7492.
(10) Mar, W.; Klein, M. L. Molecular Dynamics Study of the Self-Assembled Monolayer Composed of S(CH2)14CH3Molecules Using an All-Atoms Model. *Langmuir* **1994**, *10* (1), 188−196.
(11) Bhatia, R.; Garrison, B. J. Phase Transitions in a Methyl-Terminated Monolayer Self-Assembled on Au{111}. *Langmuir* **1997**, *13* (4), 765−769.
(12) Rai, B.; Sathish, P.; Malhotra, C. P.; Pradip; Ayappa, K. G. Molecular Dynamic Simulations of Self-Assembled Alkylthiolate Monolayers on an Au(111) Surface. *Langmuir* **2004**, *20* (8), 3138−3144.
(13) Camillone, N.; Chidsey, C. E. D.; Liu, G.; Putvinski, T. M.; Scoles, G. Surface Structure and Thermal Motion of N-alkane Thiols Self-assembled on Au(111) Studied by Low Energy Helium Diffraction. *J. Chem. Phys.* **1991**, *94* (12), 8493−8502.
(14) Nuzzo, R. G.; Korenic, E. M.; Dubois, L. H. Studies of the Temperature-dependent Phase Behavior of Long Chain *n* -alkyl Thiol Monolayers on Gold. *J. Chem. Phys.* **1990**, *93* (1), 767−773.
(15) Fenter, P.; Eisenberger, P.; Liang, K. S. Chain-Length Dependence of the Structures and Phases of CH 3 (CH 2) n - 1 SH Self-Assembled on Au(111). *Phys. Rev. Lett.* **1993**, *70* (16), 2447−2450.
(16) Day, B. S.; Morris, J. R. Packing Density and Structure Effects on Energy-Transfer Dynamics in Argon Collisions with Organic Monolayers. *J. Chem. Phys.* **2005**, *122* (23), 234714.
(17) Day, B. S.; Morris, J. R.; Alexander, W. A.; Troya, D. Theoretical Study of the Effect of Surface Density on the Dynamics of Ar + Alkanethiolate Self-Assembled Monolayer Collisions. *J. Phys. Chem. A* **2006**, *110* (4), 1319−1326.
(18) Poirier, G. E. Characterization of Organosulfur Molecular Monolayers on Au(111) Using Scanning Tunneling Microscopy. *Chem. Rev.* **1997**, *97* (4), 1117−1128.
(19) Love, J. C.; Estroff, L. A.; Kriebel, J. K.; Nuzzo, R. G.; Whitesides, G. M. Self-Assembled Monolayers of Thiolates on Metals as a Form of Nanotechnology. *Chem. Rev.* **2005**, *105* (4), 1103−1170.
(20) Vericat, C.; Vela, M. E.; Benitez, G.; Carro, P.; Salvarezza, R. C. Self-Assembled Monolayers of Thiols and Dithiols on Gold: New Challenges for a Well-Known System. *Chem. Soc. Rev.* **2010**, *39* (5), 1805−1834.
(21) Vericat, C.; Vela, M. E.; Corthey, G.; Pensa, E.; Cortes, E.; Fonticelli, M. H.; Ibanez, F.; Benitez, G. E.; Carro, P.; Salvarezza, R. C. Self-Assembled Monolayers of Thiolates on Metals: A Review Article on Sulfur-Metal Chemistry and Surface Structures. *RSC Adv.* **2014**, *4* (53), 27730−27754.
(22) Paz, Y.; Trakhtenberg, S.; Naaman, R. Reaction between O(3P) and Organized Organic Thin Films. *J. Phys. Chem.* **1994**, *98* (51), 13517−13523.
(23) Yuan, H.; Gibson, K. D.; Li, W.; Sibener, S. J. Modification of Alkanethiolate Monolayers by O(3P) Atomic Oxygen: Effect of Chain Length and Surface Temperature. *J. Phys. Chem. B* **2013**, *117* (16), 4381−4389.
(24) Feulner, P.; Niedermayer, T.; Eberle, K.; Schneider, R.; Menzel, D.; Baumer, A.; Schmich, E.; Shaporenko, A.; Tai, Y.; Zharnikov, M. Strong Temperature Dependence of Irradiation Effects in Organic Layers. *Phys. Rev. Lett.* **2004**, *93* (17), 178302.
(25) Sayler, J. D.; Brown, S.; Sibener, S. J. Chain-Length-Dependent Reactivity of Alkanethiolate Self-Assembled Monolayers with Atomic Hydrogen. *J. Phys. Chem. C* **2019**, *123* (44), 26932−26938.
(26) Mantis Deposition Ltd. MCG75 Thermal Gas Cracker Operations Manual, 2017.
(27) Nečas, D.; Klapetek, P. Gwyddion: An Open-Source Software for SPM Data Analysis. *Cent. Eur. J. Phys.* **2012**, *10* (1), 181−188.
(28) Gorham, J.; Smith, B.; Fairbrother, D. H. Modification of Alkanethiolate Self-Assembled Monolayers by Atomic Hydrogen: Influence of Alkyl Chain Length. *J. Phys. Chem. C* **2007**, *111* (1), 374−382.
(29) Kautz, N. A.; Kandel, S. A. Alkanethiol Monolayers Contain Gold Adatoms, and Adatom Coverage Is Independent of Chain Length. *J. Phys. Chem. C* **2009**, *113* (44), 19286−19291.
(30) Kautz, N. A.; Kandel, S. A. Alkanethiol/Au(111) Self-Assembled Monolayers Contain Gold Adatoms: Scanning Tunneling Microscopy before and after Reaction with Atomic Hydrogen. *J. Am. Chem. Soc.* **2008**, *130* (22), 6908−6909.
(31) Kautz, N. A.; Fogarty, D. P.; Kandel, S. A. Degradation of Octanethiol Self-Assembled Monolayers from Hydrogen-Atom Exposure: A Molecular-Scale Study Using Scanning Tunneling Microscopy. *Surf. Sci.* **2007**, *601* (15), L86−L90.
(32) Kautz, N. A.; Kandel, S. A. Reactivity of Self-Assembled Monolayers: Local Surface Environment Determines Monolayer Erosion Rates. *J. Phys. Chem. C* **2012**, *116* (7), 4725−4731.
(33) Lee, D. Y.; Kautz, N. A.; Kandel, S. A. Reactivity of Gas-Phase Radicals with Organic Surfaces. *J. Phys. Chem. Lett.* **2013**, *4* (23), 4103−4112.
(34) Poirier, G. E.; Pylant, E. D. The Self-Assembly Mechanism of Alkanethiols on Au(111). *Science* **1996**, *272* (5265), 1145−1148.
(35) Fitts, W. P.; White, J. M.; Poirier, G. E. Low-Coverage Decanethiolate Structure on Au(111): Substrate Effects. *Langmuir* **2002**, *18* (5), 1561−1566.
(36) Poirier, G. E.; Fitts, W. P.; White, J. M. Two-Dimensional Phase Diagram of Decanethiol on Au(111). *Langmuir* **2001**, *17* (4), 1176−1183.
(37) Poirier, G. E. Coverage-Dependent Phases and Phase Stability of Decanethiol on Au(111). *Langmuir* **1999**, *15* (4), 1167−1175.
(38) Mulder, W. H.; Calvente, J. J.; Andreu, R. A Kinetic Model for the Reductive Desorption of Self-Assembled Thiol Monolayers. *Langmuir* **2001**, *17* (11), 3273−3280.
(39) Poirier, G. E.; Tarlov, M. J. Molecular Ordering and Gold Migration Observed in Butanethiol Self-Assembled Monolayers Using Scanning Tunneling Microscopy. *J. Phys. Chem.* **1995**, *99* (27), 10966−10970.
(40) Doudevski, I.; Hayes, W. A.; Schwartz, D. K. Submonolayer Island Nucleation and Growth Kinetics during Self-Assembled Monolayer Formation. *Phys. Rev. Lett.* **1998**, *81* (22), 4927−4930.
(41) Vinokurov, I. A.; Morin, M.; Kankare, J. Mechanism of Reductive Desorption of Self-Assembled Monolayers on the Basis of Avrami Theorem and Diffusion. *J. Phys. Chem. B* **2000**, *104* (24), 5790−5796.
(42) Dordi, B.; Schönherr, H.; Vancso, G. J. Reactivity in the Confinement of Self-Assembled Monolayers: Chain Length Effects on the Hydrolysis of *N* -Hydroxysuccinimide Ester Disulfides on Gold. *Langmuir* **2003**, *19* (14), 5780−5786.
(43) Waring, C.; Bagot, P. A. J.; Bebbington, M. W. P.; Räisänen, M. T.; Buck, M.; Costen, M. L.; McKendrick, K. G. How Penetrable Are Thioalkyl Self-Assembled Monolayers? *J. Phys. Chem. Lett.* **2010**, *1* (13), 1917−1921.
(44) Turner, D. A.; Schalk, C. N.; Kandel, S. A. Atomic Hydrogen Reactions of Alkanethiols on Au(111): Phase Transitions at Elevated Temperatures. *J. Phys. Chem. C* **2020**, *124* (13), 7139−7143.

https://doi.org/10.1021/acs.jpcc.1c07487
J. Phys. Chem. C XXXX, XXX, XXX−XXX